Journal of Power Sources 255 (2014) 355–359

Contents lists available at ScienceDirect

Journal of Power Sources

journal homepage: www.elsevier.com/locate/jpowsour

Short communication

Boron doping at P-site to improve electrochemical performance of $LiMnPO_4$ as cathode for lithium ion battery

C.L. Hu [a,b], H.H. Yi [b], F.X. Wang [a], S.Y. Xiao [a], Y.P. Wu [a,c,*], D. Wang [c], D.L. He [c]

[a] New Energy and Materials Laboratory (NEML), Department of Chemistry & Shanghai Key Laboratory of Molecular Catalysis and Innovative Materials, Fudan University, Shanghai 200433, China
[b] School of Chemical and Material Engineering, Hubei Polytechnic University, Huangshi 435003, China
[c] National Engineering Research Center for Nanotechnology, Shanghai 200241, China

HIGHLIGHTS

- A boron doped $LiMnPO_4$ on P-site, $LiMn(P_{0.9}B_{0.1}O_{4-\delta})$, was synthesized using a simple solid state method.
- Diffusion of lithium ions is improved and charge transfer resistance is decreased.
- $LiMn(P_{0.9}B_{0.1}O_{4-\delta})$ shows better electrochemical performance compared to the virginal $LiMnPO_4$.
- The discharge capacity of $LiMn(P_{0.9}B_{0.1}O_{4-\delta})$ is 43% higher than that of the virginal $LiMnPO_4$.
- There is no capacity fading after 50 cycles.

ARTICLE INFO

Article history:
Received 20 September 2013
Received in revised form
8 December 2013
Accepted 10 December 2013
Available online 17 December 2013

Keywords:
Lithium ion battery
Lithium manganese phosphate
Cathode
Doping
Electrochemical behavior

ABSTRACT

To improve the electrochemical performance of $LiMnPO_4$ cathode for lithium ion battery, many efforts focus on cation doping/substitution on Mn-site. Here we synthesize a boron doped $LiMnPO_4$ on P-site, $LiMn(P_{0.9}B_{0.1}O_{4-\delta})$, by a simple solid-state method. It is characterized by X-ray diffraction, scan electron microscopy, cyclic voltammograph, electrochemical impedance spectroscopy and capacity testing. Results show that its electrochemical performance is improved compared with the virginal $LiMnPO_4$. It delivers a capacity of about 130 mAh g^{-1} at 0.1 C and remains 71% of the capacity at high discharge rate of 2 C. After 50 cycles at 0.2 C, there is no evident capacity fading.

1. Introduction

Lithium manganese phosphate is a promising cathode material for lithium ion batteries due to the advantages of low cost, high energy density and environmental friendliness. It offers a redox potential of 4.1 V vs. Li^+/Li, which is compatible with the presently available commercial electrolytes and higher than that of $LiFePO_4$ [1,2]. However, $LiMnPO_4$ also suffers from extremely poor electrochemical activity attributed to its low intrinsic electronic conductivity and slow lithium diffusion kinetics [2–4]. Therefore, many efforts have been made to overcome these problems by carbon coating [5–8], decreasing particle size [7–12] and ion doping or substitution [13–18].

Ion doping is an effective way to improve the electrochemical performance of some electrode materials for lithium ion batteries including $LiMnPO_4$ [13–18]. Various cation doped $LiMn_{1-x}M_xPO_4$ materials have been reported [15–25]. The introduction of doping ions obviously enhances the electronic conductivity, and hence high discharge capacity and good rate capability can be obtained for the doped $LiMnPO_4$. Up to now, all reports focused on the Mn-site doping with cation [16–28], and there is little report on anion doping/substitution for $LiMnPO_4$ at P-site. In the case of the well-studied $LiFePO_4$, there are only reports for the anion doping at oxygen-site by fluorine or chlorine [29,30].

In the present work, B-doped $LiMnPO_4$ materials at the P-site were synthesized by a simple solid-state reaction route. Results

* Corresponding author. New Energy and Materials Laboratory (NEML), Department of Chemistry & Shanghai Key Laboratory of Molecular Catalysis and Innovative Materials, Fudan University, Shanghai 200433, China.
E-mail addresses: wuyp@fudan.edu.cn, wuyuping99@yahoo.com (Y.P. Wu).

0378-7753/$ – see front matter © 2013 Elsevier B.V. All rights reserved.
http://dx.doi.org/10.1016/j.jpowsour.2013.12.040

show that boron doping can significantly improved the electrochemical performance of the $LiMnPO_4$.

2. Experimental

B-doped $LiMn(P_{0.9}B_{0.1}O_{4-\delta})$ was prepared by solid-state reaction using LiH_2PO_4, $Mn(CH_3COO)_2{\cdot}4H_2O$, $LiBO_2{\cdot}8H_2O$ and sucrose as raw materials, in which the molar ration of Li:Mn:P:B was 1:1:0.9:0.1. These raw materials were mixed by ball-milling for 6 h and then heated at 600 °C for 10 h under Ar atmosphere. For comparison, virginal $LiMnPO_4$ and $LiMn(P_{1-x}B_xO_{4-\delta})$ with various B/P ratios (3/7, 5/5 and 9/1) materials were synthesized by the similar way.

The two samples were characterized by X-ray diffraction (XRD, D8 Advance of Bruker) utilizing Cu K_α radiation. The morphology and particle size of the samples were observed by scan electron microscopy (SEM, SEM515 of Philips). Thermal analysis of the two samples was performed on an SDT-Q600 instrument under air flow to test the amount of carbon.

Electrochemical measurement was carried out by the assembly of 2016 coin-type cell with lithium metal foil as the counter and reference electrode. The working electrode was made by mixing the prepared $LiMnPO_4$ or $LiMn(P_{0.9}B_{0.1}O_{4-\delta})$, Super P and polyvinylidene fluoride (PVDF) in a weight ratio of 8:1:1. A solution of 1 M $LiPF_6$ in a 1:1:1 mixture of ethylene carbonate (EC), dimethyl carbonate (DMC) and ethyl methyl carbonate (EMC) was used as the electrolyte. All cells were assembled in an Ar-filled glove box. Cells were tested at a constant current–constant voltage (CC–CV) mode from 2.0 to 4.5 V. Cyclic voltammetric (CV) test was recorded between 2.0 and 4.7 V at a scan rate of 0.05 mV s^{-1}. Electrochemical impedance spectroscopy (EIS) was carried out in a frequency range from 100 mHz to 100 kHz with an AC signal of 5 mV.

3. Results and discussion

The XRD patterns of the virginal $LiMnPO_4$ and $LiMn(P_{0.9}B_{0.1}O_{4-\delta})$ are shown in Fig. 1. All the diffraction peaks of the two samples can be indexed to the olivine $LiMnPO_4$ phase and no impure phase was observed. Once more P was substituted by B, high B/P ratios will lead to the formation of impurities such as $Mn_3(BO_3)_2$, Li_3PO_4 and $LiMnBO_3$ and even generate pure phase $LiMnBO_3$ in the products as shown in Fig. S1. From the patterns in Fig. 1, broad diffraction peaks with low intensities are found, indicating that the crystallinity for both materials is not high because of low heat-treatment temperature and the presence of carbon. Substitution of partial P by B in $LiMnPO_4$ results in a decrease of the peak intensity and an increase of the full width at half maximum. Based on the well-known Scherrer equation, their crystal parameters were calculated. In the case of $LiMn(P_{0.9}B_{0.1}O_{4-\delta})$, a, b, c and the cell volume are 6.088 Å, 10.515 Å, 4.707 Å and 301.33 $Å^3$, respectively. In the case of the virginal $LiMnPO_4$, they are 6.105 Å, 10.458 Å, 4.748 Å and 303.16 $Å^3$, respectively. This means that B-doping at P-site for $LiMnPO_4$ leads to smaller crystal size, which is due to the smaller covalent radius of B (0.082 nm) than that of P (0.106 nm). In addition, the B-doping leads to less amount of oxygen, which is also one reason for the smaller crystal size.

The results from the thermal analysis show that the carbon amount in the B-doped and virginal $LiMnPO_4$ are about 15 wt.%, as shown in Fig. 2. It is known that the behavior of $LiMnPO_4$ is similar to that of $LiFePO_4$, and carbon is essential to achieve good electrochemical performance. However, the absence of carbon diffraction peak in the XRD patterns shows that the carbon pyrolyzed from $MnC_4H_6O_4$ and sucrose is amorphous due to the low heat-treatment temperature.

SEM micrographs of the virginal $LiMnPO_4$ and B-doped $LiMnPO_4$ are shown in Fig. 3. Some reports showed that ion doping could change the morphology of $LiMnPO_4$ [17–19]. Here our prepared virginal $LiMnPO_4$ and B-doped $LiMnPO_4$ have similar particle size and distribution from the SEM images. They consist of submicron particles with size range of 200–600 nm. Carbon from the decomposition of acetate and sucrose not only acts as a conductive additive but also suppresses the crystal growth during heating process.

EIS is an important technology to the study of lithium ion batteries. Fig. 4a shows the Nyquist plots of $LiMnPO_4$ and $LiMn(P_{0.9}B_{0.1}O_{4-\delta})$, which were obtained from a two-electrode coin cell after activation by 5 full cycles. The two plots present a similar profile composed of a semicircle in a high-to-medium frequency and an inclined line in the low frequency. An equivalent circuit as shown the inset of Fig. 4a is used to fit the impedance spectrum. The elements of R_s, CPE_{ct}, R_{ct} and Z_w represent the solution resistance, charge-transfer resistance, double-layer capacitance and Warburg impedance, respectively. The fitting results shows that the charge-transfer resistance decreases from 159.8 Ω in virginal $LiMnPO_4$ to 96.7 Ω in $LiMn(P_{0.9}B_{0.1}O_{4-\delta})$ due

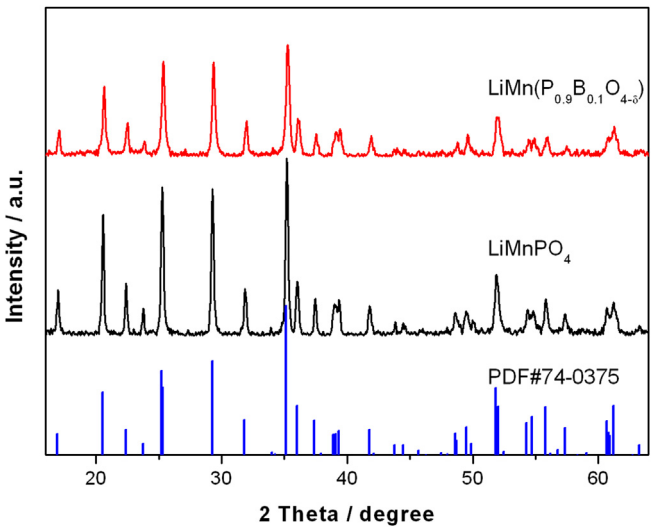

Fig. 1. XRD patterns of $LiMnPO_4$ and $LiMn(P_{0.9}B_{0.1}O_{4-\delta})$.

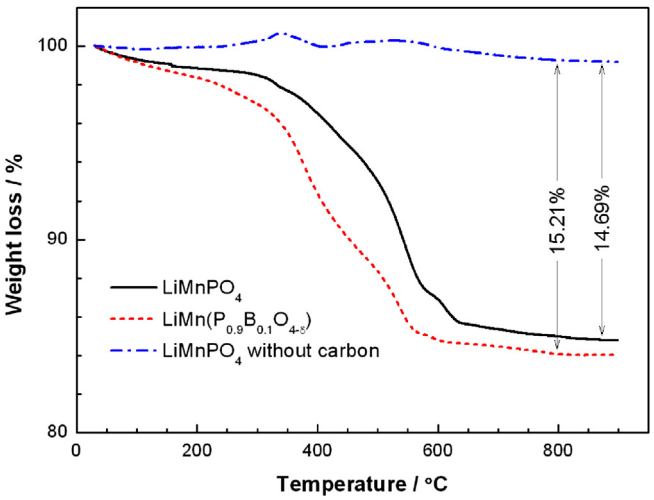

Fig. 2. TG curves of carbon coated $LiMnPO_4$ and $LiMn(P_{0.9}B_{0.1}O_{4-\delta})$, and $LiMnPO_4$ without carbon under air atmosphere (heating rate: 10 °C min^{-1}).

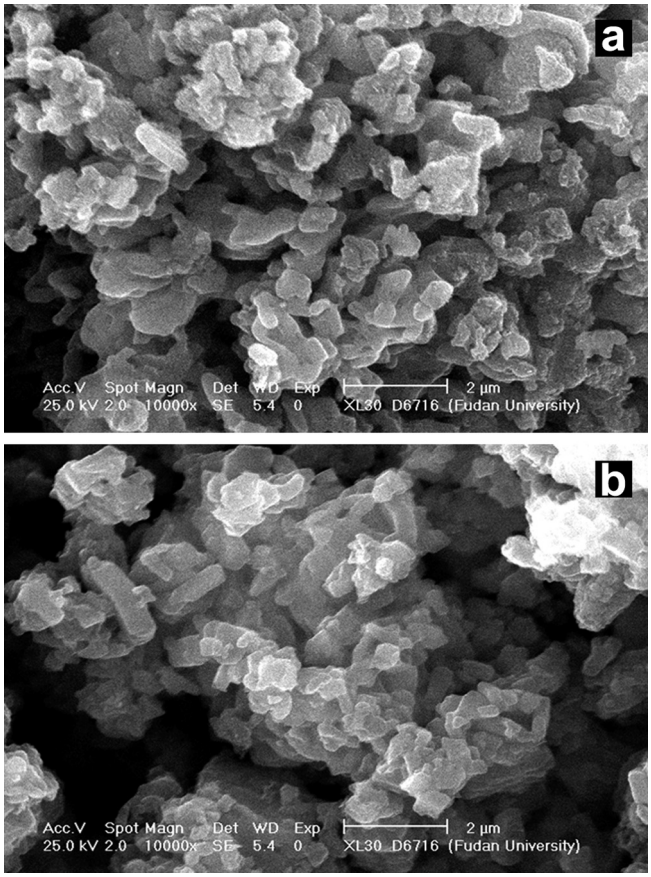

Fig. 3. SEM micrographs of (a) $LiMnPO_4$ and (b) $LiMn(P_{0.9}B_{0.1}O_{4-\delta})$.

to an enhancement in electrochemical kinetics of $LiMnPO_4$. According to the equation of $D = R^2T^2/(2n^4F^4C^2\sigma^2)$ and the linear relationship between Z' and square root of frequency ($\omega^{1/2}$) in the low-frequency region (Fig. 4b), lithium ion diffusion coefficient can also be roughly calculated from the EIS data [31]. The diffusivity of lithium ions in virginal $LiMnPO_4$ is 6.84×10^{-15} cm^2 s^{-1} whereas it is 4.02×10^{-14} cm^2 s^{-1} in B-doped sample. The above observations demonstrate that boron doping facilitates charge transfer and lithium ion diffusion.

From the CV curves at the scan rate of 0.05 mV s^{-1} (Fig. 5a), it can be seen that both materials have a redox Mn^{3+}/Mn^{2+} reaction coupled with the lithium ion extraction/insertion in the olivine structure. In the case of the virginal $LiMnPO_4$, its redox peaks are situated at 3.715 and 4.562 V, respectively. In contract, the redox peaks for the $LiMn(P_{0.9}B_{0.1}O_{4-\delta})$ are situated at 3.827 and 4.393 V, respectively. In addition, the $LiMn(P_{0.9}B_{0.1}O_{4-\delta})$ exhibits larger response. The peak separations are 0.847 V and 0.566 V for $LiMnPO_4$ and $LiMn(P_{0.9}B_{0.1}O_{4-\delta})$, respectively. This indicates that $LiMn(P_{0.9}B_{0.1}O_{4-\delta})$ presents smaller overpotential during the redox reaction and will possess an ameliorated electrochemical performance compared to the virginal $LiMnPO_4$.

Boron doping obviously improved the electrochemical performance of $LiMnPO_4$ and thus an enhancement in rate capability is expected. Fig. 5b shows the rate performance of virginal and B-doped $LiMnPO_4$ that the cells were charged galvanostatically to 4.5 V, holding the voltage until current decrease to 0.01 C, and then discharged at various rates to 2.5 V. The discharge capacities are about 100 and 130 mAh g^{-1} for $LiMnPO_4$ and $LiMn(P_{0.9}B_{0.1}O_{4-\delta})$ at 0.1 C. Boron doping leads to an increase of 30% in the discharge capacity. As the discharge rate increases from 0.1 to 2 C, $LiMn(P_{0.9}B_{0.1}O_{4-\delta})$ exhibits better rate capability. At 2 C, the discharge capacity of $LiMn(P_{0.9}B_{0.1}O_{4-\delta})$ reaches 91.5 mAh g^{-1} with a capacity retention of 71% while the capacity of $LiMnPO_4$ is only 39.6 mAh g^{-1} with a capacity retention of 40%. Therefore, boron doping can considerably improve the electrochemical performance of $LiMnPO_4$. In addition, $LiMn(P_{0.9}B_{0.1}O_{4-\delta})$ can recover its capacity when a low rate of 0.1 C is applied after the rate test, which demonstrates good electrode stability. In contrast, slight capacity decay is observed in the virginal $LiMnPO_4$. Of course, more B-doping will result in poor electrochemical performance due to the presence of inactive $Mn_3(BO_3)_2$ and Li_3PO_4 and low active $LiMnBO_3$. As shown in Fig. S2, the capacities decreased rapidly with the increase of B except the material of $LiMn(P_{0.1}B_{0.9}O_{4-\delta})$.

Charge and discharge curves of virginal and B-doped $LiMnPO_4$ are shown in Fig. 5c. The two samples reveal a flat voltage plateau of about 4.1 V at a low discharge rate of 0.1 C, indicating a two-phase reaction. After partial P is substituted for B, however, the width of the plateau increases and the voltage difference between charge and discharge plateau (ΔV) decreases obviously. Smaller ΔV means less polarization in the cell system. This is consistent with the above results from the CV curves. As the discharge rate increases to 1 C, big polarization is observed for the two samples, but B-doped $LiMnPO_4$ still displays higher discharge capacity and smaller polarization.

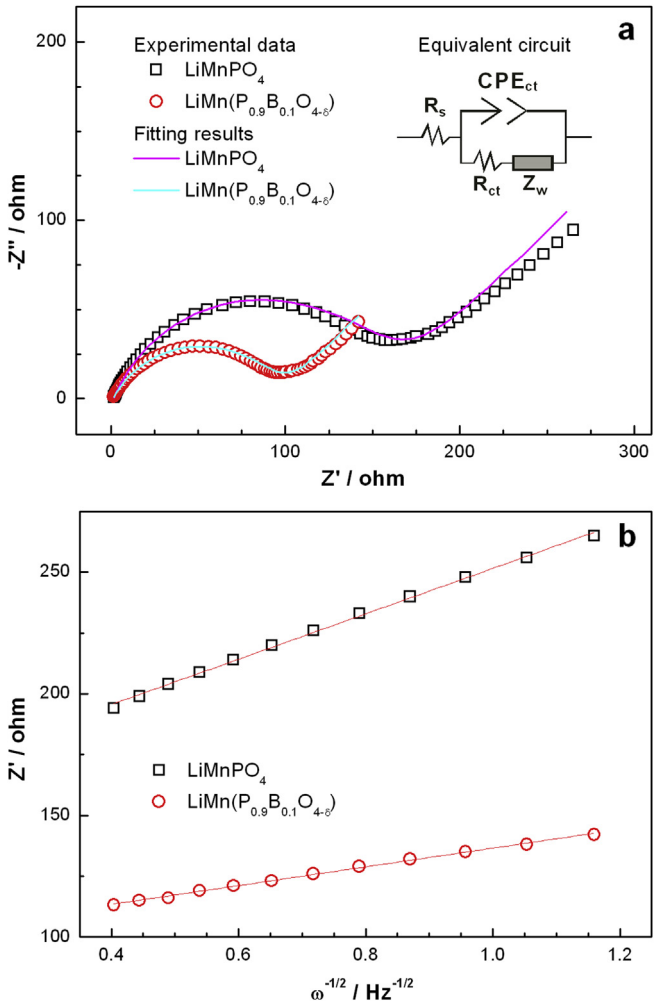

Fig. 4. Impedance spectra of $LiMnPO_4$ and $LiMn(P_{0.9}B_{0.1}O_{4-\delta})$: (a) Nyquist plots and equivalent circuit; (b) the relationship between Z' and $\omega^{-1/2}$ in the low frequency region.

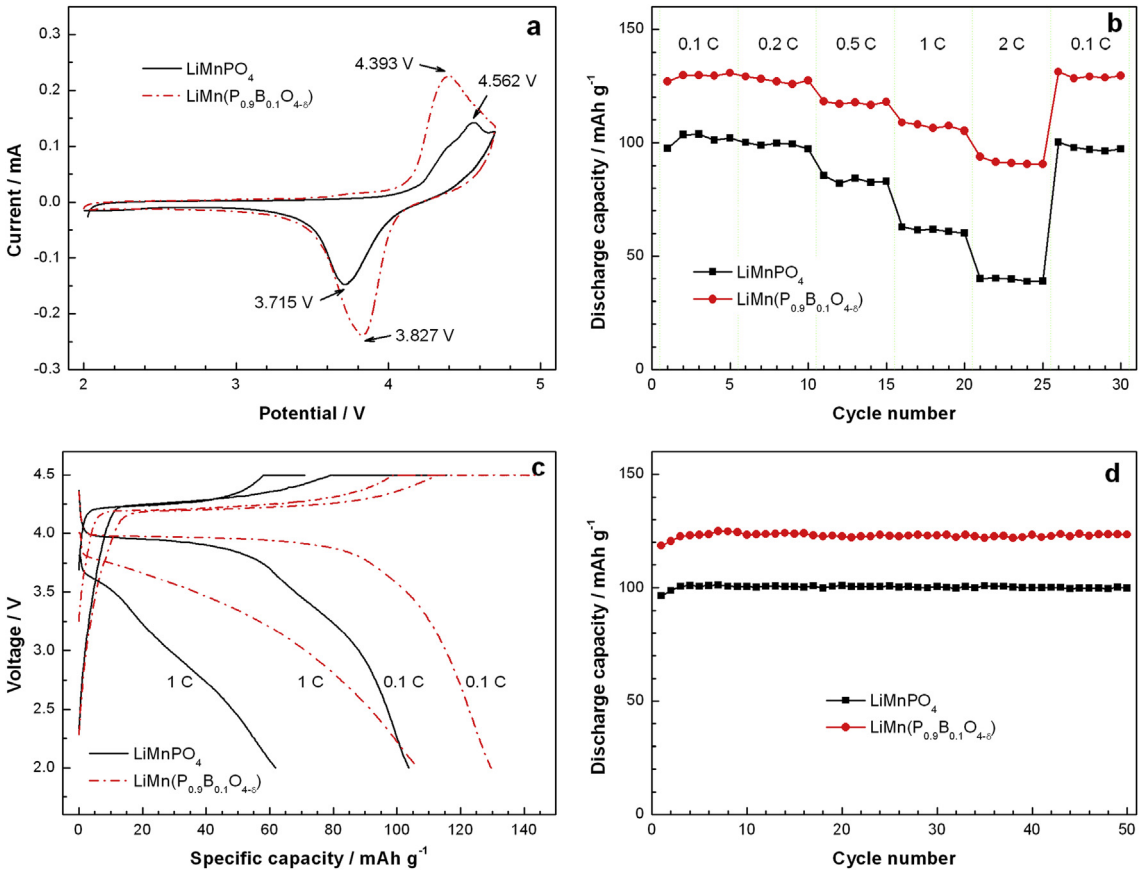

Fig. 5. Electrochemical performance of $LiMnPO_4$ and $LiMn(P_{0.9}B_{0.1}O_{4-\delta})$: (a) CV curves, (b) discharge capacities at various rates, (c) charge–discharge curves at 0.1 C and 1 C and (d) cycling performance at 0.2 C.

In rate test, B-doped $LiMnPO_4$ demonstrates good electrode stability (Fig. 5b). To further confirm its stability, charge/discharge cycling was carried out at 0.2 C for the virginal and B-doped $LiMnPO_4$, which is shown in Fig. 5d. Slight capacity increases in the first several cycles are attributed to the electrodes activation, but no obvious capacity loss is observed for the two samples after 50 cycles. This result proves that B-doped $LiMnPO_4$ also has good cycling performance.

4. Conclusions

B-doped $LiMnPO_4$ materials were synthesized by a simple solid-state reaction method and the electrochemical performance of $LiMnPO_4$ is significantly improved by substituting B for 10 atom% P. It exhibits good electrode stability and high rate capability compared with virginal $LiMnPO_4$. The discharge capacities of $LiMnPO_4$ could be increased 30% at 0.1 C and 131% at 2 C by boron doping. There is no evident capacity fading after 50 cycles at 0.2 C.

Acknowledgments

Financial support from International Science & Technology Cooperation Program of China (2010DFA61770 and 2012DFG11660), STCSM (09QH1400400) and NSFC (21073046) is gratefully acknowledged.

Appendix A. Supplementary data

Supplementary data related to this article can be found at http://dx.doi.org/10.1016/j.jpowsour.2013.12.040.

References

[1] N.H. Kwon, T. Drezen, I. Exnar, I. Teerlinck, M. Isono, M. Graetzel, Electrochem. Solid-State Lett. 9 (2006) A277–A280.
[2] V. Aravindan, J. Gnanaraj, Y. Lee, S. Madhavi, J. Mater. Chem. A 1 (2013) 3518–3539.
[3] M. Yonemura, A. Yamada, Y. Takei, N. Sonoyama, R. Kanno, J. Electrochem. Soc. 151 (2004) A1352–A1356.
[4] C. Delacourt, L. Laffont, R. Bouchet, C. Wurm, J.B. Leriche, M. Morcrette, J.M. Tarascon, C. Masquelier, J. Electrochem. Soc. 152 (2005) A913–A921.
[5] G.H. Li, H. Azuma, M. Tohda, Electrochem. Solid-State Lett. 5 (2002) A135–A137.
[6] S.M. Oh, S.W. Oh, C.S. Yoon, B. Scrosati, K. Amine, Y.K. Sun, Adv. Funct. Mater. 20 (2010) 3260–3265.
[7] J.L. Liu, X.Y. Liu, T. Huang, A. Yu, J. Power Sources 229 (2013) 203–209.
[8] K. Su, F. Liu, J.T. Chen, J. Power Sources 232 (2013) 234–239.
[9] B. Kang, G. Ceder, J. Electrochem. Soc. 157 (2010) A808–A811.
[10] D. Choi, D. Wang, I. Bae, J. Xiao, Z. Nie, W. Wang, V.V. Viswanathan, Y.J. Lee, J. Zhang, G.L. Graff, Z. Yang, J. Liu, Nano Lett. 10 (2010) 2799–2805.
[11] L. Dimesso, C. Forster, W. Jaegermann, J.P. Khanderi, H. Tempel, A. Popp, J. Engstler, J.J. Schneider, A. Sarapulova, D. Mikhailova, L.A. Schmitt, S. Oswald, H. Ehrenberg, Chem. Soc. Rev. 41 (2012) 5068–5080.
[12] X. Rui, X. Zhao, Z. Lu, H. Tan, D. Sim, H.H. Hng, R. Yazami, T.M. Lim, Q. Yan, ACS Nano 7 (2013) 5637–5646.
[13] O. Clemens, M. Bauer, R. Haberkorn, M. Springborg, H.P. Beck, Chem. Mater. 24 (2012) 4717–4724.
[14] Y.Z. Dong, H. Xie, J. Song, M.W. Xu, Y.M. Zhao, J.B. Goodenough, J. Electrochem. Soc. 159 (2012) A995–A998.
[15] A.K. Padhi, K.S. Nanjundaswamy, J.B. Goodenough, J. Electrochem. Soc. 144 (1997) 1188–1194.
[16] V. Ramar, P. Balaya, Phys. Chem. Chem. Phys. 15 (2013) 17240–17249.
[17] G.Y. Chen, J.D. Wilcox, T.J. Richardson, Electrochem. Solid-State Lett. 11 (2008) A190–A194.
[18] D.Y. Wang, C.Y. Ouyang, T. Drézen, I. Exnar, A. Kay, N.H. Kwon, P. Gouerec, J.H. Miners, M.K. Wang, M. Grätzel, J. Electrochem. Soc. 157 (2010) A225–A229.
[19] C.L. Hu, H.H. Yi, H.S. Fang, B. Yang, Y.C. Yao, W.H. Ma, Y.N. Dai, Electrochem. Commun. 12 (2010) 1784–1787.

[20] S.K. Martha, J. Grinblat, O. Haik, E. Zinigrad, T. Drezen, J.H. Miners, I. Exnar, A. Kay, B. Markovsky, D. Aurbach, Angew. Chem. Int. Ed. 48 (2009) 8559–8563.
[21] T. Shiratsuchi, S. Okada, T. Doi, J.I. Yamaki, Electrochim. Acta 54 (2009) 3145–3151.
[22] J. Kim, D.H. Seo, S.W. Kim, Y.U. Park, K. Kang, Chem. Commun. 46 (2010) 1305–1307.
[23] Z. Bakenov, I. Taniguchi, J. Electrochem. Soc. 157 (2010) A430–A436.
[24] J.W. Lee, M.S. Park, B. Anass, J.H. Park, M.S. Paik, S.G. Doo, Electrochim. Acta 55 (2010) 4162–4169.
[25] G. Yang, H. Ni, H.D. Liu, P. Gao, H.M. Ji, S. Roy, J. Pinto, X.F. Jiang, J. Power Sources 196 (2011) 4747–4755.
[26] H.H. Yi, C.L. Hu, H.H. Fang, B. Yang, Y.H. Yao, W.H. Ma, Y.N. Dai, Electrochim. Acta 56 (2011) 4052–4057.
[27] J.F. Ni, L.J. Gao, J. Power Sources 196 (2011) 6498–6501.
[28] H.S. Fang, H.H. Yi, C.L. Hu, B. Yang, Y.C. Yao, W.H. Ma, Y.N. Dai, Electrochim. Acta 71 (2012) 266–269.
[29] X.Z. Liao, Y.S. He, Z.F. Ma, X.M. Zhang, L. Wang, J. Power Sources 174 (2007) 720–725.
[30] C.S. Sun, Y. Zhang, X.J. Zhang, Z. Zhou, J. Power Sources 195 (2010) 3680–3683.
[31] H. Liu, C. Li, H.P. Zhang, L.J. Fu, Y.P. Wu, H.Q. Wu, J. Power Sources 159 (2006) 717–720.